

# A KAN-BASED LIGHTWEIGHT MODALITY FUSION METHOD FOR VIDEO-TEXT RETRIEVAL

005 **Anonymous authors**

006 Paper under double-blind review

## ABSTRACT

011 Different from the text-to-text retrieval tasks, video-text retrieval is significantly  
 012 affected by the inherent modality difference between high-dimensional visual and  
 013 textual data, which limits the model performance. Therefore, increasing works  
 014 adopted the modality fusion techniques to effectively improve the model accuracy,  
 015 while the attention mechanism from the Transformer is widely adopted to improve  
 016 the accuracy. However, the high quadratic computational complexity from the at-  
 017 tention mechanism generates the prohibitive memory cost, which is the obstacle to  
 018 the effective training on the machine and inference stage in the real world. There-  
 019 fore, to tackle the challenge, this paper proposes KFusion to fuse text and video  
 020 frames with lower computational cost, achieved by employing the Kolmogorov-  
 021 Arnold-Network-based Bridge module and Text-Frame Mamba. Bridge captures  
 022 the cross-modal feature via the learnable spline-based activation functions. It cal-  
 023 culates the weights for the text and video to facilitate the video-text fusion, but the  
 024 unimportant information from the text and video hampers the fusion effect. There-  
 025 fore, Text-Frame Mamba contains separate Mamba backbones, which is proposed  
 026 to remove the noise from the important text and frame embeddings through the  
 027 state space models. The weight vectors calculated by the Bridge multiply the fil-  
 028 tered information processed by the Mamba backbones. The performances on the  
 029 MSRVT, MSVD and Didemo benchmark datasets demonstrate the state-of-the-  
 030 art performance of KFusion in terms of the accuracy and efficiency.

## 1 INTRODUCTION

034 Video-text retrieval (VTR) is a critical task in the multi-modal understanding, divided into video-to-  
 035 text and text-to-video retrieval. Thanks to the surge of the online video, VTR has been attracting a  
 036 significant attention. The models in VTR retrieves the relevant text descriptions for videos given the  
 037 cross-modal similarity, and vice versa.

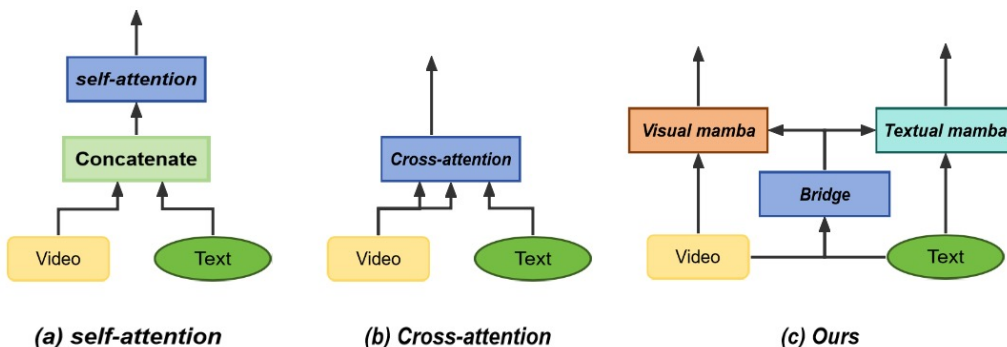


Figure 1: Architecture and performance comparisons of modality fusion methods, including self-  
 attention, cross-attention, and our proposed KFusion.

054 Current VTR research mainly adopted dual-stream and single-stream model. The single-stream  
 055 modelsDzabraev et al. (2021) achieved higher accuracy by jointly processing the visual and textual  
 056 inputs, but the issue of the computation efficiency hampered their scalability. Meanwhile, the dual-  
 057 stream architectures process the visual and textual modalities independently. Those works Zhu  
 058 & Yang (2020) outperformed the single-stream model in the VTR in terms of the efficiency, but  
 059 the insufficient interaction between the text and video limit the accuracy compared to the single-  
 060 stream models. However, since the emergence of the CLIP Radford et al. (2021) pre-trained on  
 061 400-million image-text pairs has changed the paradigm due to its zero-shot performance. Thereby,  
 062 increasing research began to fine-tune on the CLIP, and they significantly outperformed non-CLIP-  
 063 based approaches Dzabraev et al. (2021); Li et al. (2022).

064 However, the zero-shot ability of the CLIP is still constrained by the inherently-huge modality gap  
 065 between visual and textual representations that degrades the accuracy of the alignment. To bridge  
 066 the gap between the text and video, as shown in Figure 1, many researchers adopted attention mech-  
 067 anism from Transformer Vaswani et al. (2017) to fuse the visual information and text and achieved  
 068 higher accuracy, mainly divided into the cross-attention and self-attention. Those works that fuse the  
 069 textual and visual embedding Chen et al. (2023); Wu et al. (2023) took the concatenated the textual  
 070 and visual embedding as the input to the self-attention. Those works Wang et al. (2024); Jin et al.  
 071 (2023b;a); Gorti et al. (2022) that applied cross-attention used the text as the query vector, and the  
 072 visual embedding as the key and value vectors to make the visual embedding fused with the textual  
 073 information.

074 However, in the stage of the real-world inference and the fine-tuning on the datasets, the interaction  
 075 between the text and video leads to a high memory usage. The attention mechanism from the  
 076 Transformer inevitably suffers from the quadratic space complexity, which limits the further feasible  
 077 exploration on the use of Transformer regarding the modality fusion.

078 Therefore, this paper proposes the KFusion adopting Mamba and Vim as the backbone to fuse the  
 079 modality, consisting of a Bridge based on the Kolmogorov-Arnold Network (KAN)Liu et al. (2024)  
 080 and the Text-Frame Mamba.

081 Compared to the attention mechanism, KAN is a lightweight module that generate lower memory  
 082 consumption. KAN calculates the weight vectors for the text and video, achieved by processing the  
 083 joint text and video. The weight vectors for the text and video is multiplied with the filtered text and  
 084 video features. However, KAN is insensitive to the positional information that captures the relative  
 085 position of the text and video frames. Therefore, the positional information of the text and video  
 086 frames will be respectively injected given the relative positions into the text and video embedding  
 087 before the concatenation.

088 However, the modality weights are affected by the noisy features from the text and video, hampering  
 089 the effect of the modality fusion, which can also be shown in table 4. Therefore, to optimize the  
 090 effect of fusion, it is necessary to filter the less contributory information.

091 As the aforementioned disadvantage regarding the computational efficiency, the filtration of the  
 092 irrelevant information is necessary. Recently, MambaGu & Dao (2023) achieved superior accuracy  
 093 over Transformer with linear computational space complexity. Mamba was first used in 1-D textual  
 094 and DNA information modeling. Subsequently, increasing works Zhu et al. (2024); Li et al. (2024);  
 095 Tang et al. (2024); Liu et al. (2025) also extended Mamba to the 2-D computer vision and even  
 096 multi-modal downstream tasks.

097 Bridge replaces the residual connections from the original Mamba and Vim branch. Text-Frame  
 098 Mamba applies the textual Mamba based on Mamba Gu & Dao (2023) for 1-D text and visual  
 099 Mamba based on Vim Zhu et al. (2024) for 2-D sampled video frames as the backbone to optimize  
 100 the textual and visual features from via the state space models (SSM), respectively. As shown in  
 101 the Table 4, applying the separate Mamba frameworks shows the higher accuracy over the way  
 102 that using two identical Mamba framework. The experimental result demonstrated the advantage of  
 103 using modality-specific Mamba backbones in the multi-modal domain.

104 The main contributions can be summarized as follows:

105 (1) The Bridge integrates the relative positional information to produce the weights to fuse the video  
 106 and text, along with the filtered features produced from the Text-Frame Mamba.

108 (2) This Text-Frame is proposed to remove the noisy text and video features through the state space  
 109 models. KFusion includes the modality-specific Mamba backbones for the effectiveness to discard  
 110 the insignificant video and text features.

111 (3) Evaluated on extensive benchmark datasets, KFusion demonstrates the effectiveness to fuse the  
 112 modality with the consideration of the efficiency.

114

## 115 2 RELATED WORKS

116

### 117 2.1 VIDEO-TEXT RETRIEVAL

118 Followed the emergence of the CLIP Radford et al. (2021), CLIP4Clip Luo et al. (2022) endeavored  
 119 to fine-tune the CLIP on the video-text benchmark and demonstrates the better performance  
 120 compared to the previous non-CLIP-based works because of the outstanding zero-shot ability of  
 121 the CLIP. Subsequent works Liu et al. (2022); Ma et al. (2022); Wang et al. (2022) replaced the  
 122 coarse-grained alignment from the CLIP4Clip with the fine-grained alignment between the text and  
 123 video, which improved the accuracy of the model. XCLIP Ma et al. (2022) proposed the attention  
 124 over similarity matrix to calculate the similarity between the global and local representation.  
 125 DRL Wang et al. (2022) proposed the weighted-token-wise maximum based on the mean max strat-  
 126 egy from the Colbert Khattab & Zaharia (2020). Besides, The video representation is aggregated  
 127 by the video frame embeddings. Nonetheless, not every frame contributes equally. Thus, works  
 128 Wang et al. (2022); Buch et al. (2022); Liu et al. (2023); Fang et al. (2022) advanced the temporal  
 129 modeling to weight more contributory frames. However, the aforementioned works did not reduce  
 130 the modality gap, which inherently impairs the performance in every multi-modal tasks. Since the  
 131 modality fusion is an effective approach to mitigate the modality gap, works Wang et al. (2024);  
 132 Jin et al. (2023a); Gorti et al. (2022) adopted the cross-attention mechanism based on the attention  
 133 mechanism to integrate the textual information into the video frames. TABLE Chen et al. (2023)  
 134 concatenated the text information with the video frames then fed to the self-attention. Those works  
 135 outperform the CLIP-based works that do not fuse the modality. However, the attention mechanism  
 136 from the transformer inevitably leads to the high memory consumption, which will compromise  
 137 the computational efficiency in the training and inference stage. Therefore, this paper adopts a  
 138 Kolmogorov-Arnold-Network-based Bridge combined with Mamba to fuse the modality.

139

### 140 2.2 MAMBA

141

Mamba was first adopted in the language tasks, outperforming the Transformer in terms of the  
 142 accuracy with the less complexity and parameters. The state space model (SSM) from the Mamba  
 143 capture the important information from a long-range sequence. Subsequently, researchers Zhu et al.  
 144 (2024); Liu et al. (2025) exploited the Mamba backbone and proposed the bidirectional mamba,  
 145 extending the Mamba to the 2-D computer vision task. VideoMamba Li et al. (2024) followed the  
 146 similar theories Radford et al. (2021); Dosovitskiy et al. (2020); Zhu et al. (2024), which extended  
 147 the Mamba to the 3-D video understanding. Muse Tang et al. (2024) is integrated with a residual  
 148 network to model the joint resolution to produce the visual features, using the Vim Zhu et al. (2024).  
 149 VMamba Liu et al. (2025) proposed a four-way scanning mechanism tailored for spatial domain  
 150 traversal, enabling each image patch to gain contextual knowledge exclusively via a compressed  
 151 hidden state computed along the corresponding scanning path. MambaSODZhan et al. (2025) fused  
 152 the RGB and Depth through replacing the linear layers used for the residual connection with the  
 153 SSM branch, but they reside in the similar embedding space, which is not feasible to adopt the  
 154 theory in the video-text or image-text works. Thereby, this work proposes Mamba and Vim as  
 155 the backbones to filter the unnecessary information from the text and video, respectively, which  
 significantly increased the accuracy compared to the widely-used attention mechanism.

156

157

158

159 3 METHODOLOGY  
 160 As shown in the Figure 2, this section elaborates the architecture of the KFusion, including the  
 161 video and text encoder in Section 3.1, the Bridge to fuse the modality in Section 3.2, the Text-Frame  
 Mamba in the Section 3.3, and the training objective in Section 3.4.

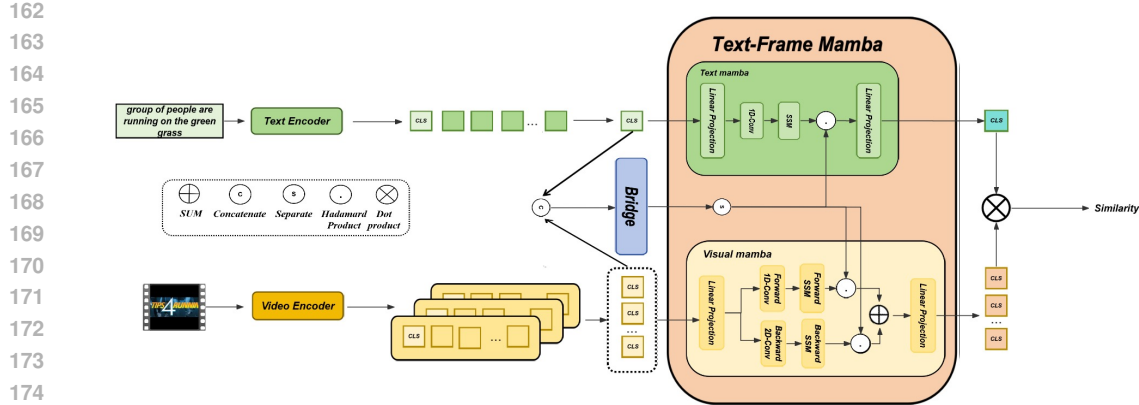


Figure 2: The model architecture of the KFusion, which includes the video encoder, text encoder, Bridge and Text-Frame Mamba.

### 3.1 VIDEO AND TEXT ENCODER

KFusion utilizes a lower-case byte pair encoding (BPE) tokenizer with a vocabulary of 49,152 to tokenize the passage  $T = \{t_1, t_2, \dots, t_{N_t}\}$ , which is then processed using the Transformer model from the CLIP, where  $N_t$  denotes the word count from a passage. [CLS] is the global representation.

Meanwhile, the Vision Transformer (ViT) from CLIP is employed to encode sampled video frames  $F$  from  $V = \{F_1, F_2, \dots, F_{n_f}\}$ , where  $n_f$  indicates the total number of frames. Both ViT-B/32 and ViT-B/16 are employed as our Video Encoders to encode the raw video. Here,  $B$ ,  $F$  and  $E$  represent the batch size, the number of sampled frames per video, and the embedding size, respectively.

### 3.2 BRIDGE

To fuse the modalities, it is very important to apply a Bridge. As shown in Figure 2, to fuse the modalities, KFusion replaces the linear layer on the residual connection branches from the textual and visual Mamba with KAN, which outperformed MLP because of the interpretability and the mitigation on the catastrophic forgetting. Specifically, as shown in Figure 5, KAN outperforms the other models in terms of accuracy. As shown in Figure 3, before concatenating to feed to the Bridge, text and video are summed with their positional embeddings  $T_E$  and  $F_{E_i}$ , formulated as:

$$T_E = \sin\left(\frac{\text{pos}}{10000}\right) \quad (1)$$

$$F_{E_{2i+1}} = \sin\left(\frac{\text{pos}}{10000^{2i/d}}\right) \quad (2)$$

$$F_{E_{2i}} = \cos\left(\frac{\text{pos}}{10000^{2i/d}}\right) \quad (3)$$

Then,  $F_{E_i}$  and  $T_E$  are summed with the original video frame and text embeddings for further concatenation, which can be formulated as:

$$F_{iy} = F_{E_i} + F_i \quad i = 1, \dots, N \quad (4)$$

$$T_y = T_E + T \quad (5)$$

$$M = \text{concat}(T_y, F_1, F_2, \dots, F_N) \quad (6)$$

Where concat,  $T_y$ ,  $F_{iy}$ , and  $M$  denote the concatenation operation, the textual and video frame embeddings that incorporate their positional information, and the concatenated modality information, respectively. Subsequently,  $M$  will be fed to the Bridge to obtain the weight vector, which is implemented by separating the output.

KAN is applied between two layers for normalization. Different from the MLP models, KAN primarily updates the parameters from the activation functions rather than the weights, formulated as:

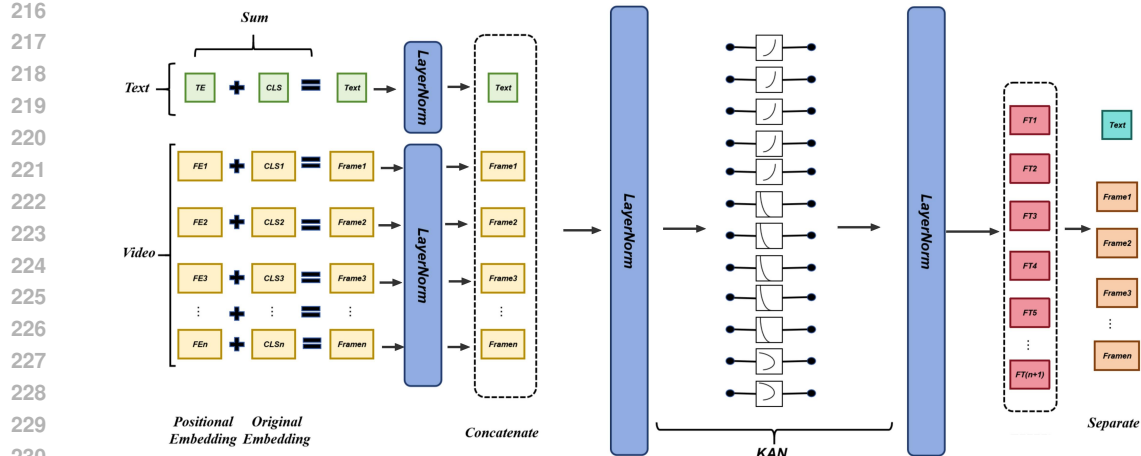


Figure 3: The Bridge is based on KAN, interleaved with several layer normalization layers. It fuses the modality between the video and text.

$$M_y = \Phi \circ M = \left[ \sum_{i=1}^{d_{in}} \phi_{i,1}(M_i) \cdots \sum_{i=1}^{d_{in}} \phi_{i,d_{out}}(M_i) \right] \quad (7)$$

where  $\Phi$  is produced by the  $\Phi_{in}$  and  $\phi_{out}$ , which can be defined as:

$$\phi = \begin{pmatrix} \Phi_1 \\ \Phi_2 \\ \vdots \\ \Phi_{2n+1} \end{pmatrix} \begin{pmatrix} \phi_{1,1} & \phi_{1,2} & \cdots & \phi_{1,2n+1} \\ \phi_{2,1} & \phi_{2,2} & \cdots & \phi_{2,2n+1} \\ \vdots & \vdots & \ddots & \vdots \\ \phi_{n,1} & \phi_{n,2} & \cdots & \phi_{n,2n+1} \end{pmatrix} \quad (8)$$

where  $\phi$  is the combination of the SiLU activation and B-Spline function, which can be formulated via the linear combination as:

$$\phi(M) = w_b \frac{M}{1 + e^{-M}} + w_s \sum_i c_i B_i(x) \quad (9)$$

Here,  $B_i(x)$  is a B-spline function.  $w_b$  and  $w_s$  denote the weight parameters, and  $c_i$  is a control coefficient to shape the B-spline that represents any univariate function on a finite domain.

After passing the KAN, the KFusion separates the concatenated text and video to obtain the weights for the text and video, which are  $w_t$  and  $w_v$ , respectively.

### 3.3 TEXT-FRAME MAMBA

Since Mamba demonstrates the better performance than transformer in terms of the memory and accuracy, as shown in Figure 2, this paper proposes Text-Frame Mamba that utilizes two modality-specific Mamba backbones to fuse the video and text.

However, different from the existing works that applied a single Mamba backbone, the Text-Frame Mamba from the KFusion leveraged the Vim Zhu et al. (2024) and Mamba Gu & Dao (2023) to respectively prioritize the more contributory information from the 1-D text and 2-D frame feature via the SSM to solve the issue of modality adaptability.

It maps the input sequence  $x_t$  and  $x_v$  to the output sequence via the hidden state  $h_t(x)$  and  $h_v(x)$ , evolution parameters  $A_t \in \mathbb{R}^{N \times N}$  and  $A_v \in \mathbb{R}^{N \times N}$ , projection parameters  $B_t \in \mathbb{R}^{N \times 1}$ ,  $B_v \in$

270  $\mathbb{R}^{N \times 1}$ ,  $C_t \in \mathbb{R}^{1 \times N}$  and  $C_v \in \mathbb{R}^{1 \times N}$ , which can be formulated as:  
 271

$$272 \quad h'_t(T) = A_t h_t(T) * B_t x_t(T) \quad (10)$$

$$274 \quad h'_v(V) = A_v h_v(V) * B_v x_v(V) \quad (11)$$

$$276 \quad T_y = C_t h(T) \quad (12)$$

$$278 \quad V_y = C_v h(V) \quad (13)$$

280 However, the parameters are continuous. Only when the parameters  $A_t, A_v, B_t$  and  $B_v$  are dis-  
 281 cretized through the timescale  $\Delta$  to produce  $\overline{A_t}, \overline{A_v}, \overline{B_t}$  and  $\overline{B_v}$ , respectively, the Mamba can be  
 282 used in the training and inference, which is calculated as:  
 283

$$284 \quad \overline{A_t} = \exp(\Delta A_t) \quad (14)$$

$$286 \quad \overline{B_t} = (\Delta A_t)^{-1}(\exp(\Delta A_t) - I)\Delta B_t \quad (15)$$

$$288 \quad \overline{A_v} = \exp(\Delta A_v) \quad (16)$$

$$290 \quad \overline{B_v} = (\Delta A_v)^{-1}(\exp(\Delta A_v) - I)\Delta B_v \quad (17)$$

292 As shown in Figure 2, since the video frame is 2-D features, the Vim Zhu et al. (2024) that proposed  
 293 the backward direction based on the Mamba is leveraged for frames. Despite this modification, the  
 294 state space models from the visual Mamba and Mamba can select the critical textual and visual  
 295 details effectively to produce  $T_y$  and  $V_y$ , respectively, which can be formulated as:  
 296

$$297 \quad T_y = T * \overline{K_t} \quad (18)$$

$$299 \quad V_y = V * \overline{K_v} \quad (19)$$

301 Where  $\overline{K_t}$  and  $\overline{K_v}$  are the coefficient convolutional details in the textual and visual mamba, respec-  
 302 tively, which can be formulated as:  
 303

$$304 \quad \overline{K_t} = (C_t \overline{B_t}, C_t \overline{A_t B_t}, \dots, C_t \overline{A_t^{L-1} B_t}, \dots, C_t \overline{A_t^{N_t-1} B_t}) \quad (20)$$

$$306 \quad \overline{K_v} = (C_v \overline{B_v}, C_v \overline{A_v B_v}, \dots, C_v \overline{A_v^{L-1} B_v}, \dots, C_v \overline{A_v^{n_f-1} B_v}) \quad (21)$$

308 Then, the refined text feature  $T_y$  and video feature  $V_y$  produced from Text-Frame Mamba, which  
 309 can be formulated as:  
 310

$$311 \quad T' = T_y \circ w_t \quad (22)$$

$$313 \quad V' = V_y \circ w_t \quad (23)$$

315 Where  $V'$  and  $T'$  are the fused video frame and text features, respectively. Then the fused video  
 316 frame embeddings will be aggregated to the overall video representation  $\overline{V'}$  via mean pooling to  
 317 produce the similarity matrix  $S(V, T)$ , which can be formulated as:  
 318

$$319 \quad \overline{V'} = \frac{1}{n} \sum_{i=1}^n V'_i \quad (24)$$

$$323 \quad S(V, T) = \frac{\overline{V'} \cdot T'}{\|\overline{V'}\| \cdot \|T'\|} \quad (25)$$

324 3.4 TRAINING OBJECTIVE  
325

326 In this study, the InfoNCE loss is applied to maximize the similarity values on the diagonal, while  
327 reducing the similarity values of unrelated pairs, which can be formulated as:  
328

$$329 \quad L_{v2t} = -\frac{1}{B} \sum_{i=1}^B \log \left( \frac{\exp(\tau \cdot s(v_i, t_i))}{\sum_{j=1}^B \exp(s(v_i, t_j))} \right) \quad (26)$$

$$332 \quad L_{t2v} = -\frac{1}{B} \sum_{i=1}^B \log \left( \frac{\exp(\tau \cdot s(v_i, t_i))}{\sum_{j=1}^B \exp(s(v_j, t_i))} \right) \quad (27)$$

335 Where  $L_{v2t}$  and  $L_{t2v}$  denote the InfoNCE loss in the video-to-text and text-to-video directions,  
336 respectively. Then, the overall objective InfoNCE loss is computed by averaging  $L_{v2t}$  and  $L_{t2v}$ :  
337

$$338 \quad L_{InfoNCE} = \frac{1}{2} (L_{v2t} + L_{t2v}) \quad (28)$$

341 Here,  $L_{InfoNCE}$  targets the optimization of cross-modal similarities, with  $B$  representing the batch  
342 size and  $\tau$  the temperature hyper-parameter.  
343

344 4 EXPERIMENT  
345346 4.1 BENCHMARK AND EVALUATION METRICS  
347

348 In this paper, to evaluate the effectiveness of the KFusion, experiments were conducted on MSRVTT  
349 Xu et al. (2016), MSVD Chen & Dolan (2011), and DiDeMoAnne Hendricks et al. (2017)datasets.  
350

351 The MSR-VTT dataset includes 10,000 videos, with a duration ranging from 10 to 32 seconds  
352 and 20 captions per video. The experiments used a training set of 9,000 videos and a test set of  
353 1,000 text-video pairs. The MSVD dataset contains 1,970 videos, with train, validation, and test  
354 splits comprising 1,200, 100, and 670 videos, respectively, and about 40 sentences per video in  
355 English. DiDeMo contains 10,000 videos annotated with 40 sentences each, concatenating all text  
356 descriptions into a single passage per video.  
357

358 Standard retrieval metrics are recall at rank K (R@K), median rank (MdR), and mean rank (MnR) ,  
359 which were used to evaluate the methodology. R@K evaluates model performance by the matched  
360 samples among the top K results. The paper used K=1,5, and 10 as retrieval criteria. MdR and MnR  
361 measure the median and mean positions of the matched results, respectively, where lower values  
362 indicate better performance.  
363

364 4.2 EXPERIMENT DETAILS  
365

366 Experiments were conducted on 8 NVIDIA GeForce RTX 4090 GPUs in 35 hours by the PyTorch  
367 library. Following practices from previous CLIP-based works, the Transformer and Vision Trans-  
368 former from CLIP are initialized as the text encoder and video encoder, respectively. The Adam  
369 optimizer is used with weight decay regularization, and the learning rate is decayed following a co-  
370 sine schedule. The initial learning rates are set as 1e-7 for the text and video encoder, and 1e-3 for  
371 other modules. The values of other parameters vary given the specific properties of a benchmark.  
372 For the maximum sentence length, we set 32 for MSR-VTT and MSVD, and 64 for ActivityNet,  
373 and Didemo. For the maximum total frames in a video, we assign 12 for MSR-VTT, MSVD, and  
374 64 for ActivityNet, and Didemo. Batch sizes are set to 256 for MSR-VTT, MSVD, and 512 for  
375 ActivityNet, and Didemo. Each benchmark is run for 5 training epochs.  
376

377 4.3 COMPARISONS TO STATE-OF-THE-ART METHODS  
378

379 Table 1 presents the performance of the KFusion on the MSRVTT dataset. In the text-to-video  
380 retrieval, when using ViT-B /32 as the backbone, the KFusion surpassed the TABLE and TS2-Net  
381 by 0.4% and 0.5% on the metric R@1, respectively. Moreover, it surpassed the X-Pool by 0.6% on  
382

it. Meanwhile, when using ViT-B/16 as the backbone, on the metric R@1, the KFusion achieved 51.8% on the text-to-video (T2V) retrieval, exceeding STAN by 1.8%, and 51.1% on the video-to-text (V2T) retrieval and overtook the UcoFiA by 2.0%.

Table 1: Performance comparison on MSRVTT dataset.

Model	R@1	Text-to-Video Retrieval				Video-to-Text Retrieval			
		R@5	R@10	MdR	MnR	R@1	R@5	R@10	MdR
<i>CLIP-based models (ViT-B/32)</i>									
CLIP4CLIP Luo et al. (2022)	44.5	71.4	81.6	2.0	15.3	42.7	70.9	80.6	2.0
X-CLIPMa et al. (2022)	46.1	73.0	83.1	2.0	13.2	46.8	73.3	84.0	2.0
XPoolGorti et al. (2022)	46.9	72.8	82.2	2.0	14.3	44.3	73.3	84.0	2.0
TS2-Net Liu et al. (2022)	47.0	74.5	83.8	2.0	13.0	45.3	74.1	83.7	2.0
TABLE Chen et al. (2023)	47.1	74.3	82.9	2.0	13.4	47.2	74.2	84.2	2.0
DRL Wang et al. (2022)	47.4	74.6	83.8	2.0	12.8	45.3	73.9	83.3	-
DiCoSAJin et al. (2023a)	<b>47.5</b>	74.7	83.8	2.0	13.2	46.7	75.2	84.3	2.0
KFusion (ViT-B/32)	<b>47.5</b>	<b>75.6</b>	<b>84.6</b>	<b>2.0</b>	<b>12.2</b>	<b>47.1</b>	<b>76.1</b>	<b>84.7</b>	<b>2.0</b>
<i>CLIP-based models (ViT-B/16)</i>									
CLIP4CLIP Luo et al. (2022)	46.4	72.1	82.0	2.0	13.3	45.4	73.4	82.4	2.0
CenterCLIPZhao et al. (2022)	48.4	73.8	82.0	2.0	13.8	47.7	75.0	83.3	2.0
X-CLIPMa et al. (2022)	49.3	75.8	84.8	2.0	12.2	48.9	<b>76.8</b>	84.5	2.0
TS2-Net Liu et al. (2022)	49.4	75.6	83.8	2.0	13.5	46.6	75.9	84.9	2.0
DRL Wang et al. (2022)	50.2	76.5	84.7	<b>1.0</b>	12.4	48.9	76.3	85.4	-
KFusion (ViT-B/16)	<b>51.8</b>	<b>78.3</b>	<b>85.8</b>	2.0	<b>10.9</b>	<b>51.1</b>	<b>76.8</b>	86.3	2.0

Table 2: Retrieval performance comparisons on MSVD dataset.

Model	Text-to-Video Retrieval			Video-to-Text Retrieval		
	R@1	R@5	R@10	R@1	R@5	R@10
CLIP4CLIP Luo et al. (2022)	46.2	76.1	84.6	56.6	79.7	84.3
DiffusionRetJin et al. (2023b)	46.6	75.9	84.1	61.9	88.3	92.9
X-CLIPMa et al. (2022)	47.1	77.8	-	60.9	87.8	-
X-PoolGorti et al. (2022)	47.2	77.4	86.0	66.4	<b>90.0</b>	94.2
CenterCLIPZhao et al. (2022)	47.3	76.9	86.0	63.5	86.4	92.6
TABLE Chen et al. (2023)	47.3	<b>77.4</b>	85.5	<b>68.9</b>	93.1	97.1
KFusion (Ours)	<b>48.0</b>	76.4	<b>87.2</b>	68.1	89.6	<b>97.3</b>

Table 3: Retrieval performance comparisons on DiDeMo dataset.

Model	Text-to-Video Retrieval			Video-to-Text Retrieval		
	R@1	R@5	R@10	R@1	R@5	R@10
CLIP4CLIP Luo et al. (2022)	43.4	70.2	80.6	43.4	69.9	80.2
X-CLIPMa et al. (2022)	45.2	74.0	-	43.1	72.2	-
DiCoSAJin et al. (2023a)	45.7	74.6	<b>83.5</b>	-	-	-
VopHuang et al. (2023)	46.4	71.9	81.5	44.4	71.8	81.8
UcoFiAWang et al. (2023)	46.5	74.8	84.4	46.0	71.9	81.5
KFusion (Ours)	<b>46.6</b>	<b>75.4</b>	82.1	<b>46.1</b>	<b>74.3</b>	<b>88.8</b>

In table 2, on the MSVD dataset, KFusion surpassed X-Pool by 0.8% on the metric R@1 and 0.3% in the T2V and V2T retrieval, respectively. In table 3, on the DideMo dataset, KFusion achieves 46.6% and 46.1% on the metric R@1 in the T2V and V2T retrieval, respectively.

Meanwhile, it shows the memory usage and accuracy of KFusion on the MSRVTT dataset compared to X-Pool that applies the cross-attention mechanism, and CLIP4Clip that does not apply any multimodal fusion approach. During the training and inference stage, even though the fusion technique from the KFusion leads to 55.2 GB and 56.8 GB higher memory consumption, respectively, the KFusion surpasses the CLIP4CLIP in terms of accuracy. Moreover, the KFusion achieves 0.6% higher accuracy with 23.2 GB lower memory usage in the inference stage. As depicted in the table, the KFusion surpasses the X-Pool with 0.8 % higher accuracy with 28.8 GB lower memory consumption in the inference stage.

Compared to MSRVTT, the datasets from DiDeMo and MSVD are much smaller, which leads to overfitting and causes Mamba to relatively lag behind the state-of-the-art models. However, the proposed KFusion demonstrates the advantages over the existing works regarding the accuracy and memory use during the inference and training stages.

432 4.4 ABLATION STUDIES  
433

434 *Modules* As shown in Table 4, this ablation study also analyzes the modules from the KFusion  
435 in contrast to the CLIP4Clip. Only applying the Bridge to fuse the modality is inferior to the  
436 CLIP4Clip. When applying different Mamba-based backbones to process the video frames and  
437 text separately without considering the modality adaptability, its performance was slightly better  
438 than applying a Mamba for text or Vim for video frames only.

439 Table 4: Performance for different modules. POS stands for the positional embedding given the  
440 modality, where  $2 \times$  stands for applying Mamba or Vim to text and video.  
441

442 Model	Text-to-Video		
	443 <b>R@1</b>	444 <b>R@5</b>	445 <b>R@10</b>
X-Pool	46.9	72.8	82.2
CLIP4Clip	43.1	70.4	80.8
+ Bridge	38.4	57.1	70.4
+ POS	40.5	63.2	74.9
+ Mamba	42.8	69.1	82.5
+ Vim	42.6	69.8	83.1
+ $2 \times$ Mamba	44.2	72.2	82.5
+ $2 \times$ Vim	42.6	68.2	78.7
+ Text-Frame Mamba	<b>47.5</b>	<b>75.6</b>	<b>84.6</b>

451 *Bridge* Apart from the KAN, this section analyzes the feasibility of self-attention and MLP to fuse  
452 the modality for the ridgebackbone. As shown in Table 5, improvement on the accuracy shows the  
453 necessities to fuse the video and text. Because of the model complexity that leads to overfitting,  
454 when applying the self-attention mechanism from the Transformer, it falls behind the MLP. KAN  
455 surpasses MLP by 0.7% on the R@1 at the text-to-video retrieval.  
456

457 Table 5: Performance comparison between the possible models that fuse the modality, where NP  
458 stands for not replacing linear layer for the residual connection.  
459

460 Module	Text-to-Video		
	461 <b>R@1</b>	462 <b>R@5</b>	463 <b>R@10</b>
MLP	46.8	75.8	84.4
self attention	46.4	75.4	83.9
KAN	47.5	75.6	84.6

465 *Layer numbers of the Text-Frame Mamba* As shown in Table 6, even though applying the Text-Frame  
466 Mamba outperforms the Transformer with regard to the accuracy and space efficiency, more layers  
467 can produce the higher accuracy. However, with the increase of the Text-Frame layers, the model  
468 accuracy started to decrease, which can be attributed to the introduction of the massive parameters  
469 that complicates the model, leading to the overfitting.  
470

471 Table 6: Performance comparison about the layer numbers of the Text-Frame Mamba

472 Layer number	Text-to-Video		
	473 <b>R@1</b>	474 <b>R@5</b>	475 <b>R@10</b>
1	47.2	<b>76.1</b>	83.8
2	<b>47.5</b>	75.6	<b>84.6</b>
3	46.9	73.3	82.3
4	45.4	68.9	80.1

## 478 480 5 CONCLUSION

481 KFusion significantly fuses the modality in video-text retrieval to achieve higher accuracy with the  
482 lower computational consumption, which is accomplished by the KAN that fuses the text and video  
483 by producing the weights, and the Text-Frame Mamba leveraging the modality-specific Mamba  
484 backbones to discard the information for the better fusion effect. The experiments on multiple  
485 benchmark datasets demonstrate that KFusion outperforms existing methods in terms of accuracy  
and computational efficiency.

486 REFERENCES  
487

488 Lisa Anne Hendricks, Oliver Wang, Eli Shechtman, Josef Sivic, Trevor Darrell, and Bryan Russell.  
489 Localizing moments in video with natural language. In *Proceedings of the IEEE international*  
490 *conference on computer vision*, pp. 5803–5812, 2017.

491 Shyamal Buch, Cristóbal Eyzaguirre, Adrien Gaidon, Jiajun Wu, Li Fei-Fei, and Juan Carlos  
492 Niebles. Revisiting the “video” in video-language understanding. In *Proceedings of the*  
493 *IEEE/CVF conference on computer vision and pattern recognition*, pp. 2917–2927, 2022.

494 David Chen and William B Dolan. Collecting highly parallel data for paraphrase evaluation. In  
495 *Proceedings of the 49th annual meeting of the association for computational linguistics: human*  
496 *language technologies*, pp. 190–200, 2011.

497 Yizhen Chen, Jie Wang, Lijian Lin, Zhongang Qi, Jin Ma, and Ying Shan. Tagging before alignment:  
498 Integrating multi-modal tags for video-text retrieval. In *Proceedings of the AAAI Conference on*  
499 *Artificial Intelligence*, volume 37, pp. 396–404, 2023.

500 Alexey Dosovitskiy, Lucas Beyer, Alexander Kolesnikov, Dirk Weissenborn, Xiaohua Zhai, Thomas  
501 Unterthiner, Mostafa Dehghani, Matthias Minderer, Georg Heigold, Sylvain Gelly, et al. An  
502 image is worth 16x16 words: Transformers for image recognition at scale. *arXiv preprint*  
503 *arXiv:2010.11929*, 2020.

504 Maksim Dzabroev, Maksim Kalashnikov, Stepan Komkov, and Aleksandr Petushko. Mdmmmt: Mu-  
505 ltidomain multimodal transformer for video retrieval. In *Proceedings of the IEEE/CVF conference*  
506 *on computer vision and pattern recognition*, pp. 3354–3363, 2021.

507 Han Fang, Pengfei Xiong, Luhui Xu, and Wenhan Luo. Transferring image-clip to video-text re-  
508 trieval via temporal relations. *IEEE Transactions on Multimedia*, 25:7772–7785, 2022.

509 Satya Krishna Gorti, Noël Vouitsis, Junwei Ma, Keyvan Golestan, Maksims Volkovs, Animesh  
510 Garg, and Guangwei Yu. X-pool: Cross-modal language-video attention for text-video retrieval.  
511 In *Proceedings of the IEEE/CVF conference on computer vision and pattern recognition*, pp.  
512 5006–5015, 2022.

513 Albert Gu and Tri Dao. Mamba: Linear-time sequence modeling with selective state spaces. *arXiv*  
514 *preprint arXiv:2312.00752*, 2023.

515 Siteng Huang, Biao Gong, Yulin Pan, Jianwen Jiang, Yiliang Lv, Yuyuan Li, and Donglin Wang.  
516 Vop: Text-video co-operative prompt tuning for cross-modal retrieval. In *Proceedings of the*  
517 *IEEE/CVF conference on computer vision and pattern recognition*, pp. 6565–6574, 2023.

518 Peng Jin, Hao Li, Zesen Cheng, Jinfa Huang, Zhennan Wang, Li Yuan, Chang Liu, and Jie Chen.  
519 Text-video retrieval with disentangled conceptualization and set-to-set alignment. *arXiv preprint*  
520 *arXiv:2305.12218*, 2023a.

521 Peng Jin, Hao Li, Zesen Cheng, Kehan Li, Xiangyang Ji, Chang Liu, Li Yuan, and Jie Chen. Dif-  
522 fusionret: Generative text-video retrieval with diffusion model. In *Proceedings of the IEEE/CVF*  
523 *international conference on computer vision*, pp. 2470–2481, 2023b.

524 Omar Khattab and Matei Zaharia. Colbert: Efficient and effective passage search via contextualized  
525 late interaction over bert. In *Proceedings of the 43rd International ACM SIGIR conference on*  
526 *research and development in Information Retrieval*, pp. 39–48, 2020.

527 Dongxu Li, Junnan Li, Hongdong Li, Juan Carlos Niebles, and Steven CH Hoi. Align and prompt:  
528 Video-and-language pre-training with entity prompts. In *Proceedings of the IEEE/CVF Confer-*  
529 *ence on Computer Vision and Pattern Recognition*, pp. 4953–4963, 2022.

530 Kunchang Li, Xinhao Li, Yi Wang, Yinan He, Yali Wang, Limin Wang, and Yu Qiao. Videomamba:  
531 State space model for efficient video understanding. In *European Conference on Computer Vision*,  
532 pp. 237–255. Springer, 2024.

533 Ruyang Liu, Jingjia Huang, Ge Li, Jiashi Feng, Xinglong Wu, and Thomas H Li. Revisiting temporal  
534 modeling for clip-based image-to-video knowledge transferring. In *Proceedings of the IEEE/CVF*  
535 *Conference on Computer Vision and Pattern Recognition*, pp. 6555–6564, 2023.

540 Yue Liu, Yunjie Tian, Yuzhong Zhao, Hongtian Yu, Lingxi Xie, Yaowei Wang, Qixiang Ye, Jianbin  
 541 Jiao, and Yunfan Liu. Vmamba: Visual state space model. *Advances in neural information*  
 542 *processing systems*, 37:103031–103063, 2025.

543 Yuqi Liu, Pengfei Xiong, Luhui Xu, Shengming Cao, and Qin Jin. Ts2-net: Token shift and selection  
 544 transformer for text-video retrieval. In *European conference on computer vision*, pp. 319–335.  
 545 Springer, 2022.

546 Ziming Liu, Yixuan Wang, Sachin Vaidya, Fabian Ruehle, James Halverson, Marin Soljačić,  
 547 Thomas Y Hou, and Max Tegmark. Kan: Kolmogorov-arnold networks. *arXiv preprint*  
 548 *arXiv:2404.19756*, 2024.

549 Huaishao Luo, Lei Ji, Ming Zhong, Yang Chen, Wen Lei, Nan Duan, and Tianrui Li. Clip4clip: An  
 550 empirical study of clip for end to end video clip retrieval and captioning. *Neurocomputing*, 508:  
 551 293–304, 2022.

552 Yiwei Ma, Guohai Xu, Xiaoshuai Sun, Ming Yan, Ji Zhang, and Rongrong Ji. X-clip: End-to-  
 553 end multi-grained contrastive learning for video-text retrieval. In *Proceedings of the 30th ACM*  
 554 *International Conference on Multimedia*, pp. 638–647, 2022.

555 Alec Radford, Jong Wook Kim, Chris Hallacy, Aditya Ramesh, Gabriel Goh, Sandhini Agarwal,  
 556 Girish Sastry, Amanda Askell, Pamela Mishkin, Jack Clark, et al. Learning transferable visual  
 557 models from natural language supervision. In *International conference on machine learning*, pp.  
 558 8748–8763. PMLR, 2021.

559 Haoran Tang, Meng Cao, Jinfang Huang, Ruyang Liu, Peng Jin, Ge Li, and Xiaodan Liang. Muse:  
 560 Mamba is efficient multi-scale learner for text-video retrieval. *arXiv preprint arXiv:2408.10575*,  
 561 2024.

562 Ashish Vaswani, Noam Shazeer, Niki Parmar, Jakob Uszkoreit, Llion Jones, Aidan N Gomez,  
 563 Łukasz Kaiser, and Illia Polosukhin. Attention is all you need. *Advances in neural informa-*  
 564 *tion processing systems*, 30, 2017.

565 Jiamian Wang, Guohao Sun, Pichao Wang, Dongfang Liu, Sohail Dianat, Majid Rabbani, Raghavveer  
 566 Rao, and Zhiqiang Tao. Text is mass: Modeling as stochastic embedding for text-video retrieval.  
 567 In *Proceedings of the IEEE/CVF conference on computer vision and pattern recognition*, pp.  
 568 16551–16560, 2024.

569 Xin Wang, Hong Chen, Si’ao Tang, Zihao Wu, and Wenwu Zhu. Disentangled representation learn-  
 570 ing. *arXiv preprint arXiv:2211.11695*, 2022.

571 Ziyang Wang, Yi-Lin Sung, Feng Cheng, Gedas Bertasius, and Mohit Bansal. Unified coarse-to-fine  
 572 alignment for video-text retrieval. In *Proceedings of the IEEE/CVF International Conference on*  
 573 *Computer Vision*, pp. 2816–2827, 2023.

574 Wenhao Wu, Haipeng Luo, Bo Fang, Jingdong Wang, and Wanli Ouyang. Cap4video: What can  
 575 auxiliary captions do for text-video retrieval? In *Proceedings of the IEEE/CVF conference on*  
 576 *computer vision and pattern recognition*, pp. 10704–10713, 2023.

577 Jun Xu, Tao Mei, Ting Yao, and Yong Rui. Msr-vtt: A large video description dataset for bridging  
 578 video and language. In *Proceedings of the IEEE conference on computer vision and pattern*  
 579 *recognition*, pp. 5288–5296, 2016.

580 Yue Zhan, Zhihong Zeng, Haijun Liu, Xiaoheng Tan, and Yinli Tian. Mambasod: Dual mamba-  
 581 driven cross-modal fusion network for rgb-d salient object detection. *Neurocomputing*, pp.  
 582 129718, 2025.

583 Shuai Zhao, Linchao Zhu, Xiaohan Wang, and Yi Yang. Centerclip: Token clustering for efficient  
 584 text-video retrieval. In *Proceedings of the 45th International ACM SIGIR Conference on Research*  
 585 *and Development in Information Retrieval*, pp. 970–981, 2022.

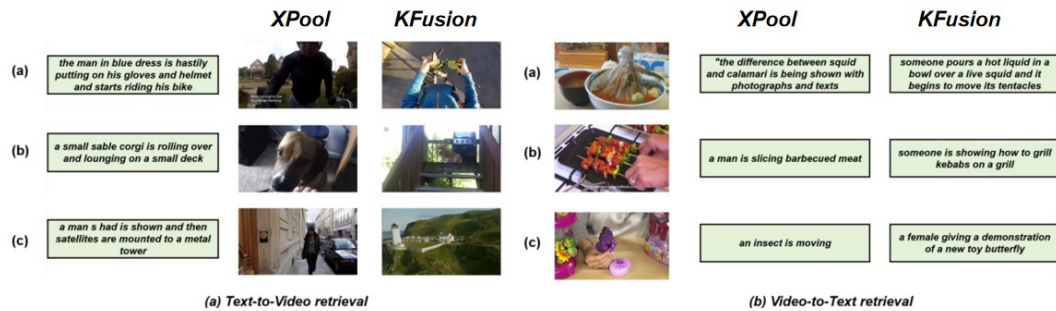
586 Lianghui Zhu, Bencheng Liao, Qian Zhang, Xinlong Wang, Wenyu Liu, and Xinggang Wang. Vision  
 587 mamba: Efficient visual representation learning with bidirectional state space model, 2024. URL  
 588 <https://arxiv.org/abs/2401.09417>.

594 Linchao Zhu and Yi Yang. Actbert: Learning global-local video-text representations. In *Proceedings*  
 595 *of the IEEE/CVF conference on computer vision and pattern recognition*, pp. 8746–8755, 2020.  
 596

597 **A APPENDIX**

599 **A.1 QUALITATIVE ANALYSIS**

600 In this section, the videos and texts are from the MSRVTT dataset, using the X-Pool for comparison.  
 601 As shown in the Figure 4, in the text-to-video retrieval, in the example (a), KFusion retrieves the  
 602 video that contains the “blue dree” and “gloves”, but no glove is shown in the video retrieved by the  
 603 X-Pool. In the example (c), KFusion retrieved the video that contains the key word “satelite”, while  
 604 X-Pool retrieved a video containing a man without the “satelite”.  
 605



618 Figure 4: The qualitative analysis via comparing KFusion with X-pool for the text-video retrieval,  
 619 divided into the text-to-video retrieval and video-to-text retrieval.  
 620

621 In the V2T retrieval, in the example (b), the text retrieved by X-pool contains “slicing” that does  
 622 not depicted in the video file, but the text retrieved by the KFusion contains “grill” and “kebabs”.  
 623 Meanwhile, in the example (c), the word “insect” and “moving” from the text retrieved by the X-Pool  
 624 were not corresponding to the video, but the “toy butterfly” from the text retrieved by the KFusion  
 625 suits more.  
 626

627  
 628  
 629  
 630  
 631  
 632  
 633  
 634  
 635  
 636  
 637  
 638  
 639  
 640  
 641  
 642  
 643  
 644  
 645  
 646  
 647